

CFD MODELLING IN THE SCALE-UP OF A STIRRED REACTOR FOR THE PRODUCTION OF RESIN BEADS

P.T.L. KOH¹ and F. XANTIDIS²

¹ CSIRO Minerals, Clayton, Victoria 3169, AUSTRALIA

² Orica Engineering Pty Ltd, Melbourne, Victoria 3000, AUSTRALIA

ABSTRACT

The manufacture of a resin made by suspension polymerization has been studied by CFD modelling. A critical stage in the manufacture of this product involves liquid-liquid dispersion of an organic phase within an aqueous system. The breakup and the subsequent polymerization determine the final droplet size distribution.

CFD modelling has been employed in scaling up a reactor for full-scale production of these resin beads. Fluid flow, organic phase distribution and turbulent dissipation rates in three stirred reactors (300 ml, 200 litre and 4 m³) have been simulated. A method has been developed for correlating the experimental particle sizes from the 300-ml and 200-litre reactors against turbulent dissipation rates obtained from the simulations. In a validation exercise, particle sizes from trials in the 200-litre reactor have been well predicted by the combined CFD and correlation method. The method was then applied to the design of a 4-m³ reactor.

NOMENCLATURE

d particle diameter
 D impeller diameter
 k turbulent kinetic energy
 s standard deviation
 T tank diameter

ε turbulent dissipation rate
 μ viscosity
 ρ density
 σ interfacial tension

INTRODUCTION

Scale-up by a factor of 20 in reactor design presents a challenge for most process designers especially when data is only available for 300-ml and 200-litre reactors. In any large scale-up process, uncertainties usually exist. To minimise the risk in proving the new process and to achieve tight plant startup deadlines a new approach was required.

Computational Fluid Dynamics (CFD) technology for numerical modelling of the complex unsteady, multi-phase, non-Newtonian flows in stirred tanks has developed to the point where it now has the capability to facilitate design of new reactors. Here, it is employed in the scale-up of the resin bead process in a full-scale

reactor. The predicted flow field and organic phase distribution in the reactor assist in better understanding of the bead production. The method is more rigorous than the compartment mixing approach used by Vivaldo-Lima *et al* (1998) for modelling suspension polymerization.

CFD modelling of the resin bead production in 300-ml laboratory, 200-litre pilot-plant and 4-m³ full-scale reactors have been performed. The dispersion stage of the process was simulated by a two-phase flow model. As the breakup of organic phase droplets is related to the local flow condition, the distributions of turbulent dissipation rates in the three reactors at various stirring speeds have been obtained from the simulations. These turbulent dissipation rates relate to the final particle size distributions in the reactors.

For correlating with CFD simulation, measured size data from the laboratory and pilot-plant reactors have been used. After testing various measurement techniques, particle size distributions obtained from the Malvern Mastersizer have been adopted. Bimodality appears in some of the size distributions under certain experimental conditions, but this is not considered in the CFD method.

Once validated, the CFD method is then applied to the design of a full-scale reactor that is to be constructed. As fundamental equations of conservation are used, the method is readily applied to any new geometry.

The chemistry of the process is kept constant for this modelling work. Laboratory work indicates that the surfactant stabiliser used in the process effectively prevents droplet re-coalescence. Heat transfer characteristics of the reaction is also not considered in this investigation.

MODEL DESCRIPTION

Unsteady two-phase flow equations for the conservation of mass, momentum and turbulence quantities have been solved using an Eulerian-Eulerian approach in which the two phases are treated as interpenetrating continua. The variables include pressure, velocity components for both phases and phase volumetric fractions. A sliding mesh technique has been used for modelling the impeller action in the stationary reactor. Based on the impeller tip speeds, the Reynolds numbers in the reactors studied indicate the flows are turbulent. The turbulent kinetic energy k and turbulent dissipation rate ε are calculated from the continuous phase velocity field and turbulence is modelled by an effective turbulent viscosity obtained from the

standard $k-\epsilon$ model (Launder and Spalding, 1974). Source terms are included to represent the generalised interactive forces between the droplet and the surrounding liquid including the standard drag and buoyancy forces. The equations were solved using the computational fluid dynamics code CFX 4.1 (1995), and time steps corresponding to 15° rotation of the impeller in the sliding mesh technique were employed.

Turbulent dissipation rate is a flow parameter that describes the rate at which mechanical energy imparted by the impeller is dissipated locally by turbulence. It is often used for calculating rates of coalescence and breakup in liquid dispersions (eg. Coualoglou *et al.*, 1977; Konno *et al.*, 1977; Pacek *et al.*, 1999). The droplet diameter during liquid breakup is governed by the flow condition described by Hinze (1955) as follows:

$$d = \text{constant} (\sigma / \rho)^{3/5} (\epsilon)^{-2/5} \quad (1)$$

where d is the maximum stable diameter, σ is the interfacial tension and ρ is density of the continuous phase. The constant in eqn (1) is dependent on the physical and chemical properties of the system. This fundamental relationship is the basis for linking the experimental size data with the turbulent dissipation rates obtained from CFD simulations.

The conditions in the simulations are similar to those used in the laboratory and pilot-plant experiments. Physical properties are taken to be at 80°C . The organic phase is denser than the aqueous phase. The shear-thinning viscosity of the organic phase is calculated using an equation obtained from experimental data. The two-phase flow was simulated initially assuming a uniform particle size of $100 \mu\text{m}$ to obtain particle drag. A turbulent Prandtl number of 1.0 was applied for the dispersion of the organic phase in the reactor.

REACTOR GEOMETRIES

Laboratory Reactor

The laboratory reactor has a volume of 300 ml, an impeller with 4 twisted blades and no baffles. The three-dimensional grid of the reactor is shown in Figure 1.

Pilot-Plant Reactor

The pilot-plant reactor (CR 250) was manufactured by Buchi Glasuster. The impeller consisting of 3 curved blades is positioned near the base of the reactor. The liquid volume is 200 litres at the dispersion stage of the process. There is a baffle consisting of three flat fingers with rounded edges. The three-dimensional grid of the reactor, including the impeller, is shown in Figure 2.

Full-Scale Reactor

The full-scale reactor is designed to have a 4-m^3 volume and an impeller consisting of four pitched blades. The grid of the proposed full-scale reactor with D/T ratio of 0.5 is shown in Figure 3.

RESULTS

Laboratory and Pilot-Plant Reactors

Simulation results including velocity vectors, distribution of the organic phase and turbulent dissipation rates in each

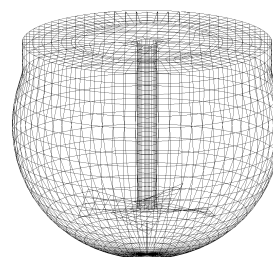


Figure 1: Grid of 300-ml laboratory reactor.

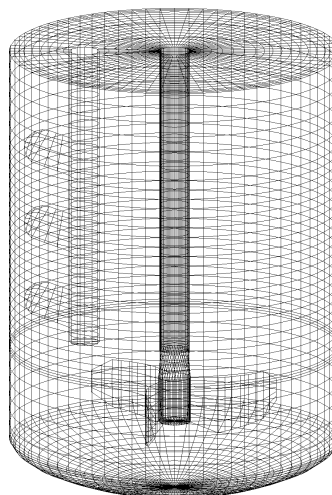


Figure 2: Grid of 200-litre pilot-plant reactor.

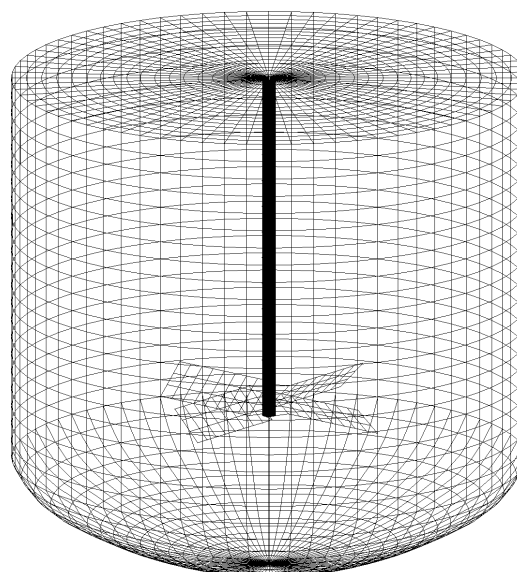


Figure 3: Grid of 4-m^3 full-scale reactor.

of the reactors have been produced at various stirring speeds. With increasing stirrer speed, the volume fraction plots indicate that the organic phase becomes more uniformly dispersed in the reactor. The organic phase fraction in the reactor is generally higher than average in the region just below the impeller. The flow in this region is however quite turbulent aiding the exchange of fluid in and out of the zone. The flow vectors are useful for studying the circulation zones in the reactor. The velocity vectors in the pilot-plant reactor indicate that there are two major recirculation zones in the tank. This is similar to the

flow patterns found in tanks stirred by Rushton turbine impellers (Lane and Koh, 1997ab).

The distribution of turbulent dissipation rates, as shown in Figure 4, is characteristic of the reactor geometry. These turbulent dissipation rates have been used to obtain the local shear rates for calculating the organic phase viscosity. Certain regions in the reactor become 'productive' when the local dissipation rate exceeds the critical value for droplet breakup as prescribed by eqn (1). To quantify the volume of productive regions for each of the three reactors studied, the cumulative distributions of turbulent dissipation rate are plotted in Figure 5. The cumulative distributions have been obtained by summing all volume elements where the dissipation rates are the same. The distribution describes essentially the spread of dissipation rates in a given reactor geometry.

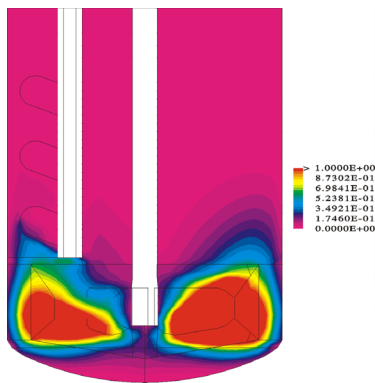


Figure 4: Distribution of turbulent dissipation rates (W/kg) in the 200-litre reactor.

In Figure 5, the distributions of turbulent dissipation rates in the laboratory and pilot-plant reactors are different because of vessel size and impeller design. For the smaller laboratory reactor, the cumulative distribution is narrower indicating that the dissipation rates are more uniform. In the pilot-plant reactor, the aspect ratio is larger with a larger region of low turbulence above the impeller.

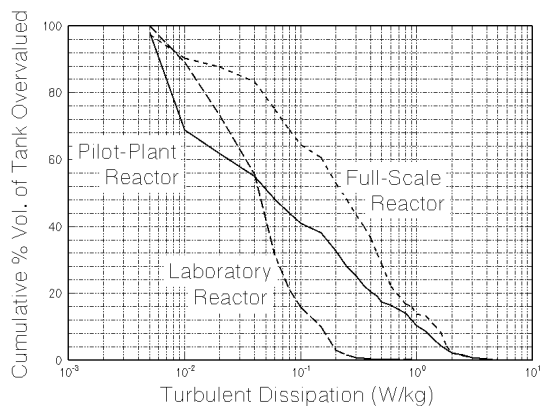


Figure 5: Cumulative distribution of turbulent dissipation rates in the laboratory reactor at 600 rpm, in the pilot-plant reactor at 108 rpm and in the full-scale reactor at 110 rpm.

Validation of Model Predictions

In the breakup mechanism of eqn (1), the final droplet size is dependent on the maximum turbulent dissipation rate in the reactor. The cumulative distributions of turbulent dissipation rates in the laboratory and pilot-plant reactors indicate that the distributions near the maximum values are very sensitive and likely to depend on grid sizes. For more accurate predictions, very fine grids requiring large computational time are needed. A maximum turbulent dissipation rate in each case can however be obtained graphically by extrapolating a fitted line over the whole distribution. In this way, a larger portion of the distribution is employed and the uncertainty in locating the maximum is reduced. From the laboratory and pilot-plant reactors, the experimental particle sizes in terms of the mean diameter and standard deviation are then correlated against the maximum turbulent dissipation rates for various stirring speeds.

From experimental size distributions for eight cases in the laboratory and pilot-plant reactors, the average diameter d_{ave} is correlated against the maximum turbulent dissipation rate ϵ_{max} as follows:

$$d_{ave} = a (\epsilon_{max})^{-b} \quad (2)$$

The correlations for the standard deviation s against the maximum turbulent dissipation rate are different in the two regions where $\epsilon_{max} < 0.3$ and $\epsilon_{max} > 0.3$ as follows:

$$(s / d_{ave}) = x + y \epsilon_{max} \quad (3)$$

where a , b , x and y are constants. Experimental and predicted values from the correlations for these eight cases are plotted in Figures 6 and 7. To validate the correlations, special experiments and CFD simulations in the pilot-

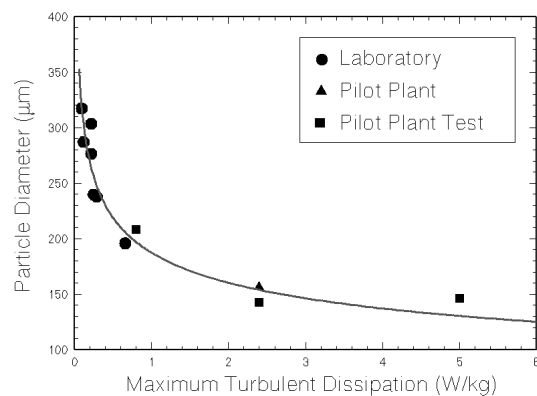


Figure 6: Experimental and predicted mean diameter of resin beads plotted against maximum turbulent dissipation rate.

plant reactor have been repeated involving three additional cases at a wider range of stirring speeds. The results of three new experimental cases are included in Figures 6 and 7, labelled as 'pilot plant test' and compared against predictions. The predicted and experimental values are in good agreement. The validation exercise provided a high degree of confidence for the methodology used to design new full-scale reactors.

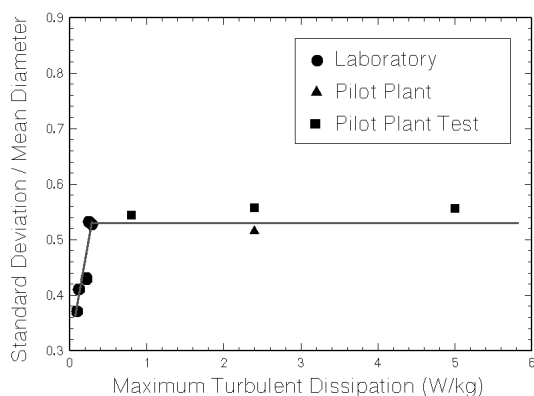


Figure 7: Experimental and predicted standard deviation of resin beads normalised by the mean diameter plotted against maximum turbulent dissipation rate.

By including the results of the additional cases for the pilot-plant reactor with the original eight cases, new correlations for the average diameter and standard deviation have been produced. Based on the experimental data for eleven cases in the laboratory and pilot-plant reactors, the correlations obtained would be an improvement over the previous correlations in eqns (2) and (3) for eight cases.

Full-Scale Reactor With D/T = 0.5

The full-scale reactor has been simulated at a stirring speed 110 rpm with a power draw of 2.0 kW. The speed has been selected to achieve the same maximum turbulent dissipation rates as in the pilot-plant reactor. Simulation results are given in the following plots: the velocity vectors in Figure 8, the distribution of the organic phase in Figure 9, the turbulent dissipation rates in Figure 10 and the cumulative distribution of turbulent dissipation rates in Figure 5. The turbulent dissipation rates in the full-scale reactor are generally greater than those obtained for the laboratory and pilot-plant reactors.

The predicted average diameter and standard deviation in the full-scale reactor is expected to be similar to those produced in the pilot-plant reactor at 108 rpm because the maximum turbulent dissipation rates are similar.

The flow vectors indicate that there are two recirculation zones in the reactor. The major flow pattern is predominantly axial. A smaller recirculating zone occurs below the impeller. With a 'liquid height to vessel diameter ratio' of 1.0, velocities near the surface are comparable to those in bulk of the reactor. The organic phase is well dispersed as shown by the narrow range in the volume fractions. In the region below the impeller, the organic fraction is not as high as that in the laboratory reactor or pilot-plant reactor, most likely as a result of higher tip speed in the full-scale reactor.

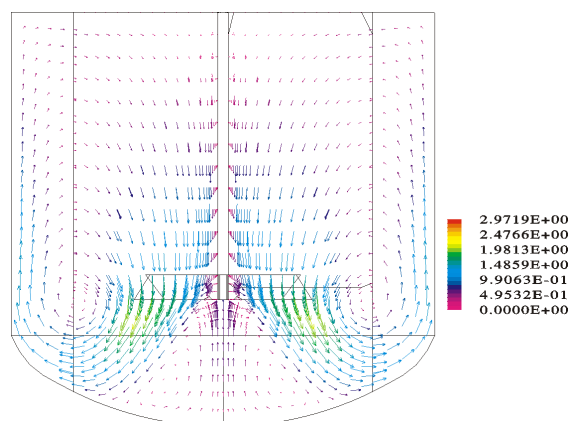


Figure 8: Velocity vectors (m/s) in the 4-m³ reactor.

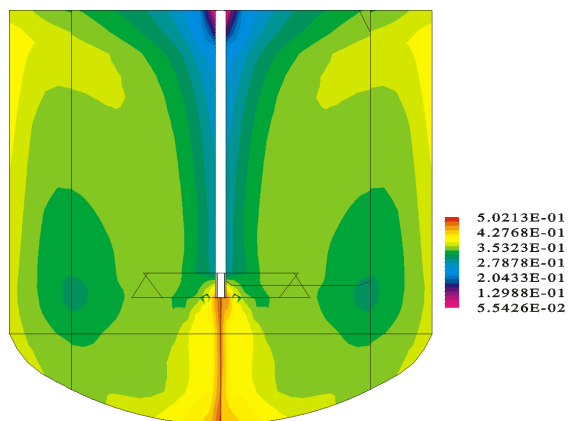


Figure 9: Distribution of volume fraction of the dispersed organic phase in the 4-m³ reactor.

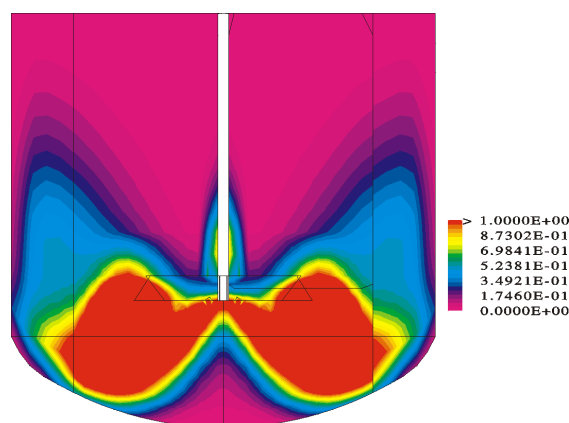


Figure 10: Distribution of turbulent dissipation rates (W/kg) in the 4-m³ reactor.

Full-Scale Reactor With D/T = 0.4

Simulations of the full-scale reactor with a smaller impeller with D/T ratio of 0.4 have been performed. The vessel volume of 4 m³ is the same as before. The impeller has four 45° pitched blades. The simulation has been performed at a stirring speed of 335 rpm. This speed has been selected to achieve similar maximum turbulent dissipation rates as in the pilot-plant reactor. The particle size distribution predicted for this reactor is expected to be similar to the particle sizes produced in the pilot-plant reactor. However, the impeller tip speed in this reactor is too high as a result of smaller impeller diameter and could affect others aspects of the process.

DISCUSSION

Baffling was not included in the full-scale reactor because it is known to assist in the buildup of organic phase in the reactor. The use of unbaffled tanks has been confirmed by correlations (Nagata, 1975) which predict the radius of cylindrically rotating zone of the forced vortex. From present CFD investigations, the mixing patterns indicate that solid body rotation is not expected to be a problem in the full-scale reactor because the swirl velocities obtained in the reactor are similar to those in the pilot-plant reactor where a baffle was used. If swirl does prove to be a problem, baffles similar to those in the pilot-plant reactor can be installed.

Buildup is known to occur even on the smooth reactor wall. The formation of particle layering on the reactor wall has been observed experimentally at high stirring speeds. It can be explained that layering occurs when partially polymerized, highly viscous and very sticky organic phase is subjected to high shear. Under this condition, deformation into flat shape particles and sticking to wall occurs. High stirring speeds are also not favoured because of the possibility of air entrainment and foaming in the reactor. A possible strategy to reduce the fouling tendency is to increase the impeller power number. This has the effect of allowing the rotational and tip speeds to be reduced whilst maintaining the maximum turbulent dissipation rate. Possible strategies include adding more blades to the impeller, increasing the pitch angle, high efficiency impellers or multiple rotors. CFD modelling of any such changes is useful since the overall flow pattern would be affected.

In the CFD model, the liquid surface is assumed to be flat. At moderate stirring speeds, this assumption of the liquid surface is not expected to have much effect because droplet breakup is an impeller-based process dependent on the shear intensity of the impeller. While droplet coalescence is a tank-bulk process which normally occurs in the quiescent regions of the tank. The presence of the surfactant stabiliser used in the process effectively prevents droplet coalescence.

The mean diameter and standard deviation of the resins produced in the pilot-plant and full-scale reactors are affected by the maximum dissipation rates. The cumulative distributions of turbulent dissipation rates in the reactors are somewhat different: wider distribution in the pilot-plant reactor but narrower distribution in the full-

scale reactor. Since the droplet breakup occurs by the impeller action, the turbulent dissipation rates associated with the breakup process have values close to the maximum value in the distribution. The other section of the distribution, away from the maximum, consists of dissipation rates in the quiescent regions of the tank where the droplet breakup do not occur. These lower dissipation rates in the bulk do not affect the main breakup processes occurring near the impeller.

For breakup processes without droplet coalescence, the width of the distribution of the turbulent dissipation rates does not affect the mean particle size. This is confirmed by experimental data in the laboratory and pilot-plant reactors where similar mean diameters have been produced with similar maximum dissipation rates even though the widths of the distributions in Figure 5 are different.

As circulation paths in the reactor increases with reactor size, the time for the dispersion process to complete needs to be adjusted if required. From the predicted flow field, an estimate of the circulation time can be obtained by taking the longest circulation path and dividing it by the average velocity. In larger reactors, the circulation times and paths both increase. This increase in circulation time is likely to produce a wider distribution of particle sizes and is the likely explanation for the different values of the standard deviation in Figure 7 for the laboratory and pilot-plant reactors. For a given dispersion time, the number of passes decreases in the larger reactor. The dispersion time cannot be increased indefinitely because the polymerization reactions could be well advanced preventing further breakup before the droplets are fully dispersed.

The application of a static mixer to replace the stirred tank in the production of an emulsion was discussed by Tattersson (1994). Similarity based on energy dissipation rates has been suggested. According to Tattersson, the time to reach equilibrium droplet size in a static mixer is usually much less in comparison to that in a stirred tank. If a static mixer is to be used, buildup of solids in the mixer caused by polymerization needs to be considered.

CONCLUSIONS

Numerical simulation has been performed on resin bead production in the 300-ml laboratory, 200-litre pilot-plant and 4-m³ full-scale reactors. Fluid flow, organic phase distribution and turbulent dissipation rates in the reactors have been obtained. A major advance in this project is the development of a method for correlating the experimental particle sizes against maximum turbulent dissipation rates obtained from CFD simulations. Size data from existing laboratory and pilot-plant reactors have been used. In the validation exercise, particle size distributions obtained during special trials in the pilot-plant reactor have been well predicted by the combined method. In scaling up, the selection of stirring speed should not be based on the impeller tip speed but on the maximum turbulent dissipation rate.

REFERENCES

- CFX USER GUIDE, Release 4.1*, (1995) Computational Fluid Dynamics Services, AEA Industrial Technology, Harwell Laboratory, Oxfordshire, UK.
- COULALOGLOU C.A. and TAVLARIDES L.L., (1977) "Description of interaction process in agitated liquid-liquid dispersions", *Chem. Eng. Sci.*, **32**, 1289-1297.
- HINZE J.O., (1955) "Fundamentals of the hydrodynamic mechanism of splitting up in dispersion processes", *AIChEJ*, **1**, 289-295.
- KONNO M., ARAI K. and SAITO S., (1977) "The effects of viscous and inertia forces on drop breakup in an agitated tank", *J. Chem. Eng. Japan*, **10**, 474-477.
- LANE G. and KOH P.T.L., (1997a) "CFD Simulation of a Rushton Turbine in a Baffled Tank", International Conference on Computational Fluid Dynamics in Mineral and Metal Processing and Power Generation, Clayton, Victoria, July.
- LANE G. and KOH P.T.L., (1997b) "CFD Simulation of Flow in a Baffled Stirred Tank", Chemeca 97, 25th Australian and New Zealand Chemical Engineering Conference, Rotorua, NZ, September/October.
- LAUNDER B.E. and SPALDING D.B., (1974) "The numerical computation of turbulent flows", *Comp. Meths. Appl. Mech. Engng.*, **3**, 269-289.
- NAGATA S., (1975) *Mixing: Principles and Applications*, John Wiley, New York, p. 1-83.
- PACEK A.W., CHAMSART S., NIENOW A.W. and BAKKER A., (1999) "The Influence of Impeller Type on Mean Drop Size and Drop Size Distribution in an Agitated Vessel", *Chem. Eng. Sci.*, **54**, 4211-4222.
- TATTERSON G.B., (1994) *Scaleup and Design of Industrial Mixing Processes*, McGraw Hill, New York, p. 166.
- VIVALDO-LIMA E., WOOD P.E., HAMIELEC A.E. and PENLIDIS A., (1998) "Calculation of the particle size distribution in suspension polymerization using a compartment-mixing model", *Can. J. Chem. Eng.*, **76**, 495-505.